Cell and Tissue Research (2019) 377:167–176
https://doi.org/10.1007/s00441-019-03008-8

REGULAR ARTICLE

Expression of Slc35f1 in the murine brain

Jacob Farenholtz[1] · Nadine Artelt[1] · Antje Blumenthal[1] · Karlhans Endlich[1] · Heyo K. Kroemer[2] · Nicole Endlich[1] · Oliver von Bohlen und Halbach[1]

Received: 20 August 2018 / Accepted: 18 February 2019 / Published online: 13 March 2019

Abstract

The solute carrier (SLC) group of membrane transport proteins includes about 400 members organized into more than 50 families. The SLC family that comprises nucleoside-sugar transporters is referred to as SLC35. One of the members of this family is SLC35F1. The function of SLC35F1 is still unknown; however, recent studies demonstrated that SLC35F1 mRNA is highly expressed in the brain and in the kidney. Therefore, we examine the distribution of Slc35f1 protein in the murine forebrain using immunohistochemistry. We could demonstrate that Slc35f1 is highly expressed in the adult mouse brain in a variety of different brain structures, including the cortex, hippocampus, amygdala, thalamus, basal ganglia, and hypothalamus. To examine the possible roles of Slc35f1 and its subcellular localization, we used an in vitro glioblastoma cell line expressing Slc35f1. Co-labeling experiments were performed to reveal the subcellular localization of Slc35f1. Our results indicate that Slc35f1 neither co-localizes with markers for the Golgi apparatus nor with markers for the endoplasmic reticulum. Time-lapse microscopy of living cells revealed that Slc35f1-positive structures are highly dynamic and resemble vesicles. Using super-resolution microscopy, these Slc35f1-positive spots clearly co-localize with the recycling endosome marker Rab11.

Keywords Rab · Slc35 · Central nervous system · Neuron

Introduction

The solute carrier (SLC) group of membrane transport proteins includes about 400 members organized into more than 50 families (Hediger et al. 2013). The solute carrier family that comprises nucleoside-sugar transporters is referred to as SLC35 (Hediger et al. 2013). The SLC35 family consists of at least 30 molecular species in humans (Hediger et al. 2013). SLC35 family members are very hydrophobic proteins of about 320–400 amino acid residues, and they are thought to act as antiporters, transporting nucleotide sugars pooled in the cytosol into the lumen of the Golgi and/or the endoplasmic reticulum (ER) in exchange for the corresponding nucleoside monophosphates (Ishida and Kawakita 2004). In detail, the SLC35 family can be categorized broadly into six subfamilies (SLC35A-G) on the basis of their amino acid similarities (Nishimura et al. 2009; Song 2013). An expression profile study has shown that human slc35f transporter mRNAs (SLC35F1–SLC35F5) are expressed in various tissues and that slc35f1 mRNA is highly expressed in the fetal brain (Nishimura et al. 2009).

Slc35f1 is expressed postnatally in different tissues. However, the exact expression pattern is largely unknown as well as the function. In birds and mammals, slc35f1 is thought to share some functions for the preservation of viable spermatozoa in the female reservoirs (Atikuzzaman et al. 2017).

In human tissue, SLC35F1 protein is especially expressed within the brain and kidney and at moderate levels in the heart (http://www.proteinatlas.org/ENSG00000196376/normal). Concerning SLC35F1 in the human heart, mRNA expression has been confirmed (Vasan et al. 2009). In a meta-analysis of genome-wide association data, common genetic variants associated with cardiac structure and function have been analyzed. The results obtained show that the left ventricular diastolic dimension was associated with two single-nucleotide

Electronic supplementary material The online version of this article (https://doi.org/10.1007/s00441-019-03008-8) contains supplementary material, which is available to authorized users.

✉ Oliver von Bohlen und Halbach
oliver.vonbohlen@uni-greifswald.de

[1] Institute of Anatomy and Cell Biology, Universitätsmedizin Greifswald, Friedrich Loeffler Str. 23c, 17487 Greifswald, Germany

[2] Faculty of Medicine, University of Göttingen, Göttingen, Germany

polymorphisms (SNPs), presumably marking the same 6q22 locus that included C6orf204 and SLC35F1 (Vasan et al. 2009). Moreover, in a further study, an association with resting heart rate (6q22 near SLC35F1) was discovered (Eijgelsheim et al. 2010). Furthermore, Slc35F1 might be involved in the regulation of heart rate dependant of the ethnicity (Avery et al. 2017). The role of SLC35F1 in cardiac physiology, however, is currently unknown as well as its function in other organs.

Since Slc35f1 is strongly expressed in the brain, we analyzed the localization of Slc35f1 in the murine brain in detail. Moreover, by in vivo microscopy and super-resolution microscopy, we identified the dynamic and the subcellular localization of Slc35f1.

Materials and methods

Animals

Adult C57BL/6J mice of both sexes with an age of 3 to 6 months were kept in standard cages with 12 h dark/light cycle as well as with access to food and water ad libitum. All of the experimental protocols were approved by government authorities (Landesamt für Landwirtschaft, Lebensmittelsicherheit und Fischerei Mecklenburg-Vorpommern. (LALLF); 7221.3-2) and performed according to the German Animal Welfare Act of May 25, 1998, and the European Communities Council Directive of November 24, 1986 (86/609/EEC). All efforts were made to minimize suffering.

Transcardial perfusion, which utilizes the vasculature to achieve systemic delivery of fixative in the living animal, is a commonly used standard for tissue fixation. For that purpose, the animal is anesthetized, the chest wall opened, the beating heart exposed, and a needle is then inserted into the left ventricle in order to pump fixative into the systemic circuit (Kasukurthi et al. 2009). To minimize suffering, we developed a method that does not require living animals; instead, the animals will be euthanized using ether and the preparation is performed postmortem. This method has been successfully used for several years in our lab (Busch et al. 2017; Dokter et al. 2015; Freund et al. 2012; Koschützke et al. 2015) and is approved by the local government (LALLF; Reference-number 7221.3-2). Exposure to anesthetic drugs, including ketamine, midazolam, propofol, isoflurane, and chloral hydrate, can induce neuroapoptosis (for review, see Creeley and Olney 2010). Moreover, on the level of neuronal plasticity, it has been shown that isoflurane affects adult hippocampal neurogenesis (Sall et al. 2009; Stratmann et al. 2009). In addition, we have shown that isoflurane, in contrast to ether, severely affects neuronal signaling and neuronal plasticity and thus an appropriate choice of anesthetics used is an important consideration when brain plasticity is analyzed (Zschenderlein et al. 2011). Therefore, ether was used to avoid neuronal damage or alterations in neuronal plasticity and is authorized by the local government.

RNA isolation and RT-PCR

Cortical brain tissues from adult C57BL/6J mice ($n = 3$) were collected. Total RNA of mouse brain was isolated using TRI Reagent (Sigma-Aldrich, St. Louis, MO, USA) as described by the manufacturer. The synthesis of cDNA was performed using QuantiTect® Reverse Transcription Kit (Qiagen, Hilden, Germany) and 1 μg of RNA according to the manufacturer's protocol. Reaction mix lacking reverse transcriptase was used as negative control. Reverse transcription PCR (RT-PCR) was performed in the presence of 1 U/μl Taq polymerase (Peqlab, Darmstadt, Germany). The following primers were used (final concentration 0.5 μM): slc35f1 forward primer (5′- GTCTTAGGAGGAGCCACCCTGTA-3′) and Slc35f1 reverse primer (5- ATGGGGCTCTTCTTCTGTCTCC-3′) getting a specific signal at 546 bp. After an initial hold of 5 min at 95 °C for denaturation, 30 cycles were performed with 30 s at 94 °C, 40 s at annealing temperature of 64 °C, and 90 s at 72 °C. PCR products were separated on 2% ethidium bromide-stained agarose gel, which were recorded with a digitizing video system (Intas, Göttingen, Germany). The product size of 546 bp was examined using GeneRuler 100 bp DNA Ladder (0.1 μg/μl, Thermo Fisher Scientific, Waltham, MA, USA). Additionally, the sequence specificity of the amplicon was confirmed by sequencing (LGC Genomics, Berlin, Germany).

Western blot

Cells were lysed in lysis buffer (50 mM octylglucoside, 50 mM Tris, 150 mM NaCl, 10 mM $CaCl_2$, 1 mM $MgCl_2$, and 1 mM PMSF) for western blot. After incubation (4 °C, 20 min, shaker), the lysate was centrifuged (10,000*g* for 20 min at 4 °C). Thereafter, the protein-containing supernatant (20–30 μg/lane) was separated under denatured conditions using a 4–20% Mini-PROTEAN® TGX™ precast gel (Bio-Rad Laboratories, Hercules, CA, USA) and transferred to a nitrocellulose membrane by electrophoresis. Blocking (5% low-fat milk, 60 min) was followed by incubation with the primary antibody (rabbit anti-SLC35F1, HPA019576, Sigma-Aldrich, Germany). For negative control, primary Slc35f1 antibody was pre-incubated with the corresponding slc35f1 antigen (PrEST Antigen SLC35F1, APREST73313, Sigma-Aldrich) and centrifuged, and finally the supernatant was used. Antigen-antibody complexes were visualized with an HRPO-labeled anti-rabbit secondary antibody (Santa Cruz Biotechnology, Dallas, TX, USA) and a Clarity Western ECL Substrate kit (Bio-Rad Laboratories, Kabelsketal, Germany).

Expression of slc35f1 protein in the adult mouse brain

In order to avoid interferences with neuronal plasticity, mice were euthanized with ether (Zschenderlein et al. 2011) and transcardiacally perfused with phosphate-buffered saline (PBS) and afterwards with 4% paraformaldehyde (PFA) as described recently (Gebhardt et al. 2016). Paraformaldehyde-fixed brains from adult C57BL/6 mice ($n = 3$) were used for this study, and 30-μm-thick coronal sections were made using a vibratome (VT 1000, Leica, Wetzlar, Germany) and collected in 20% ethanol as described earlier in detail (Dokter et al. 2015). Sections were mounted and air-dried overnight. For the detection of Slc35F1 protein, a phosphate-buffered saline (PBS) solution containing rabbit affinity-purified anti-Slc35f1 polyclonal antibodies (1:100), 5% serum, and 0.1% Triton X was used. Visualization was performed using biotinylated anti-rabbit IgG (1:200; Dianova, Hamburg, Germany) and Cy3-conjugated streptavidin (1:2000; Dianova). Sections were rinsed again three times in PBS and then counterstained with DAPI (0.1 μg/ml). Finally, sections were embedded in Mowiol (Sigma-Aldrich). Slc35f1 immunohistochemistry was combined either with an antibody against GFAP (affinity-purified polyclonal antibodies (1:50; Santa Cruz Biotechnology)) or NeuN (polyclonal antibodies (1:100; Millipore, Darmstadt, Germany)). Visualization was done using Alexa 488-conjugated antibodies (1:400; Dianova). Sections were analyzed using an Axioplan 2 imaging microscope (Zeiss, Jena, Germany). For analysis of double-stained material, a randomly chosen region of interest (ROI 200 × 200 μm) was located within the brain and the number of stained cells within that ROI was determined. Per brain region and animal, between six ROIs were sampled and the mean cell density was determined. In the overview presented in Table 1, cell densities were grouped according the following scheme: + ≤ 10, ++ ≤ 20, +++ ≤ 30 and ++++ > 30 cells per ROI. The nomenclature used is based on a mouse brain atlas (Franklin and Paxinos 2007).

Transfection of cultured glioblastoma cells

Cells of a well-established glioblastoma cell line (U-251 MG, Cell Lines Service, Eppelheim, Germany) were used. Glioblastoma cells were maintained in RPMI 1640 (Lonza, Basel, Switzerland) supplemented with 2.0 mM L-glutamine, 1.0 mM sodium pyruvate, 10% fetal bovine serum, 100 U/ml penicillin, and 10 μg/ml streptomycin. Cells were cultivated at 37 °C and 5% CO_2 on uncoated glass cover slips. Cells were transfected by a tGFP-tagged Slc35f1 plasmid (MG206418 Origene, Rockville, MD, USA) using jetPEI (Polyplus-transfection, Illkirch, France) as described by the manufacturer. The cells were taken for experiment 24 h after transfection. Control-transfected cells (carrying only a GFP-vector) as well as cells that were treated with the transfection media were used as control. For co-localization studies, Slc35f1-transfected glioblastoma cells were stained for Rab proteins as described earlier (Blumenthal et al. 2015). Cells were fixed at room

Table 1 Relative densities of slc35f1 protein–expressing cells

	Area	Relative density
Cortex	Auditory cortex	+++
	Cingulate cortex	++
	Entorhinal cortex	++
	Motor cortex	+++
	Piriform cortex	+++
	Somatosensory cortex	+++
	Visual cortex	+++
Hippocampus	CA1	++++
	CA2	+++
	CA3	+++
	DG	++++
Amygdala	BLA	++++
	Ce	+
	LA	++
	Me	+
Basal ganglia	CPu	++++
	GP	+
	Ncl. subthalamicus	++
	SN	+
Thalamus	AD	++
	DLG	++
	LHb	–
	MHb	++
	Rt	+
	VPM/VPL	+
Hypothalamus	AHA	++
	DM	++
	MN	++++
	Ncl. arcuatus	+
	Ncl. preopticus	+
	PaV	++
	PE	+
	PH	+++
Others	CM	++++
	Ncl ruber	+
	PAG	+
	raphe nuclei	++

AD, anterodorsal thalamic nucleus; *AHA*, anterior hypothalamic area; *BLA*, basolateral nucleus of the amygdala; *Ce*, central nucleus of the amygdala; *CPu*, caudate-putamen; *DG*, dentate gyrus; *DLG*, dorsal lateral geniculate nucleus; *DM*, dorsomedial hypothalamic nucleus; *GP*, globus pallidus; *LA*, lateral nucleus of the amygdala; *LHb*, lateral habenula; *Me*, medial nucleus of the amygdala; *MHb*, medial habenula; *MN*, mammillary nucleus; *PAG*, periaqueductal gray; *PaV*, paraventricular hypothalamic nucleus; *PE*, periventricular hypothalamic nucleus; *PH*, posterior hypothalamic area; *Rt*, reticular thalamic nucleus; *SN*, substantia nigra; *VPM/VPL*, ventral posteromedial/posterolateral thalamic nucleus

temperature with 2% PFA (dissolved in a solution containing 4% sucrose, and PBS). Afterwards, cells were permeabilized for 8 min (0.3% Triton X-100 in PBS) and incubated for 45 min in blocking solution (2% fetal bovine serum, 2% bovine serum albumin, 0.2% gelatin, PBS). Antibodies against the following proteins were used: rabbit anti-Slc35f1 (Sigma-Aldrich), mouse anti-Rab5 (Santa Cruz Biotechnology), mouse anti-Rab7 (Santa Cruz Biotechnology), goat anti-Rab11 (Santa Cruz Biotechnology), mouse anti-Golgin97 (Life Technologies, Carlsbad, CA, USA), rabbit anti-PDIA3 (ER) (Sigma-Aldrich), and mouse anti-α-tubulin (Sigma-Aldrich). For visualization, Cy3-conjugated and Alexa 488-conjugated (Vector Laboratories Inc., Peterborough, United Kingdom) secondary antibodies were used.

Additionally, Slc35f1-expressing cells were used for live cell imaging. A custom build Plexiglas chamber was filled with 400 μl observation medium (RPMI 1640 w/o phenol red supplemented with 10% fetal bovine serum). The uncoated cover slips were attached, and the Plexiglas chamber was sealed. For live cell observation, an inverted laser scanning microscope was used (IRBE; Leica Microsystems) and the temperature was kept at 37 °C by using an airstream incubator (ASI 400; Nevtek, Burnsville, VA, USA).

Images and videos were taken using confocal laser scanning microscopy (Leica TCS-SP5, Leica Microsystems). For analysis, the software ImageJ (NIH, USA) and the Leica Application Suite LAS AF (Leica, Germany) were used. For the subcellular analysis, pictures were taken by the use of super-resolution microscopy SIM (structured illumination microscopy; Elyra PS1, Zeiss, Germany) as recently described (Siegerist et al. 2017).

Results

Slc35f1 is expressed in the cortex and the cerebellum of mice

To obtain insight into the putative expression of Slc35f1 in the adult murine brain, we performed RT-PCR and western blots (Fig. 1a, b). By RT-PCR analysis, we confirmed Slc35f1 expression in the cortex. A specific band with the expected size of

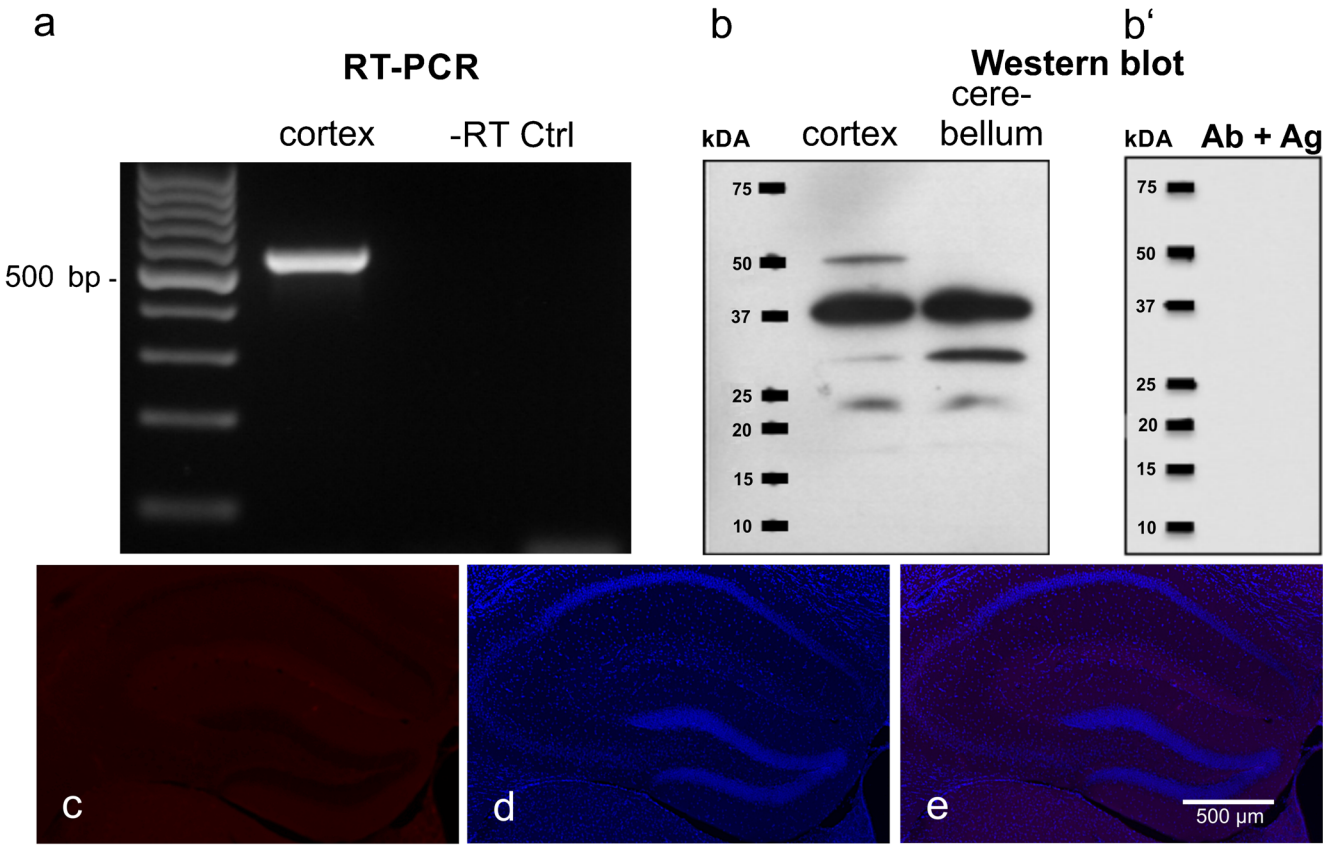

Fig. 1 Slc35f1 is expressed in the mouse brain. Slc35f1 mRNA expression in the cortical brain tissue was confirmed by RT-PCR obtaining a specific signal at 546 bp (**a**). No reverse transcriptase control (−RT Ctrl) was used as negative control. Slc35f1 protein is also detected by western blot in the cortex and the cerebellum (**b**). As a negative control (Ab+Ag), the primary Slc35f1 antibody (Ab) was pre-incubated with the slc35F1 antigen (Ag) and showed no signal (b'). Omission of the primary antibody does not result in a visible fluorescent signal (**c**), whereas the counterstaining with DAPI (in blue) clearly labels the brain structures (**d**). The overlay of (**c**) and (**d**) is shown in (**e**). RT-PCR reverse transcription PCR

45 kDa in the cortex and the cerebellum was detected by western blot, whereas the negative control showed no signal (Fig. 1b). Beside this, we could show that the antibody was also able to detect Slc35f1 in transfected glioblastoma cells expressing Slc35f1 (see below).

Distribution of Slc35f1 in the adult murine brain

Next, we used this antibody for analyzing the distribution of Slc35f1 in the adult mouse brain. The omission of the primary antibody did not reveal any specific staining on brain sections (Fig. 1c–e), whereas the use of the Slc35f1 antibody provided a specific staining pattern. In the adult murine brain, Slc35f1 protein expression is widely distributed (Fig. 2a). Slc35f1 protein was detected in most brain regions of the forebrain, including cortical, limbic, thalamic, and hypothalamic areas (Table 1). In detail, Slc35f1 protein was found to be expressed in most cortical areas. Strong Slc35f1 protein expression was mainly found in cortical layers II to VI (data not shown). Within the hippocampus, high Slc35f1 protein expression

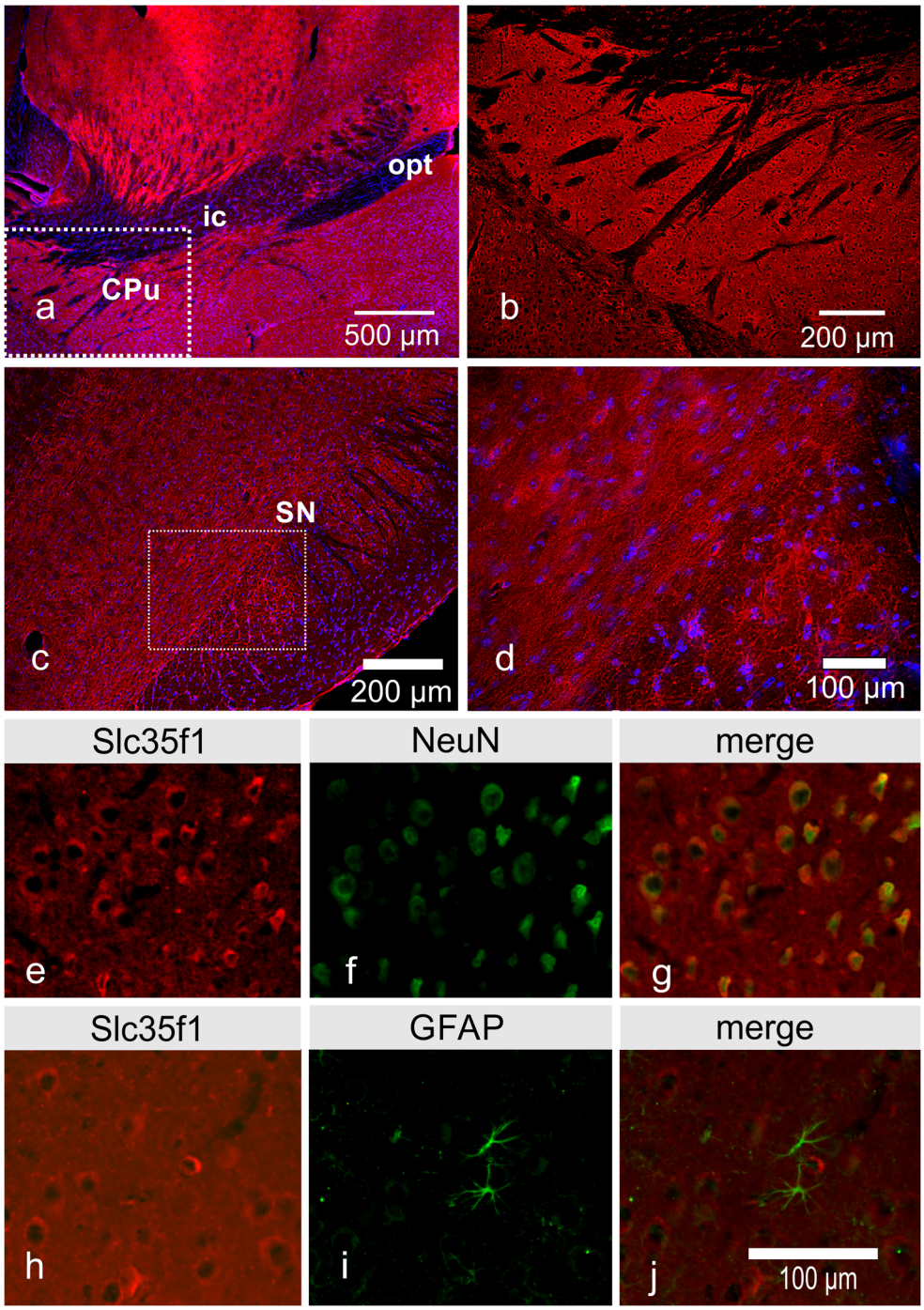

Fig. 2 Slc35f1-positive cells in the mouse brain. Within the adult mouse brain, cells positive for slc35f1 are widely distributed (**a**). A rectangle indicates a magnification of that area that is shown in (**b**). Slc35f1 is present in fibers and cells within the caudate-putamen (CPu; **b**). Slc35f1 is also expressed in the substantia nigra (**c**). Cells expressing slc35f1 protein were shown in a higher magnification (**d**). Within the cortex, slc35f1 (**e**) and NeuN (**f**) co-localize (**g**), indicating that slc35f1 is expressed by neurons. Slc35f1 (**h**) and GFAP (**i**) did not co-localize (**j**). This indicates that slc35f1 is mainly expressed by neurons. (Slc35f1 is shown in red; DAPI (in blue) was used to visualize cell nuclei). CPu caudate-putamen, fi fimbria, ic internal capsule, opt optical tract

was found, especially within area CA1 and the dentate gyrus (DG; Table 1). As compared with these hippocampal areas, the density of Slc35f1 protein–expressing cells in areas CA2 and CA3 was somewhat lower.

The most prominent expression of Slc35f1 protein was found within the basolateral complex of the amygdala, namely within the basolateral (BLA) and lateral (LA) nucleus of the amygdala. Slc35f1 protein was also found within brain areas belonging to the basal ganglia, including the subthalamic nucleus, the globus pallidus (GP). The highest density of such cells was noted in the caudate-putamen (CPu; Table 1, Fig. 2a, b). Within both, the thalamus and the hypothalamus, Slc35f1 protein–expressing cells could also be detected. The analysis of the densities of labeled cells indicated that high densities could be found within the hypothalamus especially within the mammillary nucleus (MN) and the posterior hypothalamic area (PH), whereas the densities of Slc35f1 protein–expressing cells was somewhat lower in the other areas analyzed (Table 1). Moreover, Slc35f1 protein expression was detected in other brain structures, including the nucleus ruber, substantia nigra (SN; Fig. 2c, d), periaqueductal gray (PAG), and the raphé nuclei (Table 1). According to the morphology of the Slc35f1-positive cells, these cells appear to represent neurons. This was verified by co-staining with antibodies directed against the neuronal marker NeuN (Fig. 2e–g). In order to investigate whether Slc35f1 protein is also expressed by glial cells, immunohistochemistry for Slc35f1 was combined with immunohistochemistry for GFAP. These double-labeling experiments showed that GFAP-positive cells were not positive for Slc35f1 (Fig. 2h–j). Along this line, Slc35f1 expression was not seen in fiber tracts, e.g., optical tract or internal capsule (Fig. 2b).

Moreover, by using fluorescence microscopy, Slc35f1 is not only identified in neuronal somata, but also in dendrites (Fig. 3a, b). Likewise, by using SIM (structured illumination microscopy, a super-resolution microscopic technique), a spot-like expression pattern of Slc35f1 was seen in neurons. The expression of Slc35f1 protein was seen in the soma as well as in dendrites (Fig. 3c).

Cellular localization of slc35f1

SLC35 family members are thought to transport nucleotide sugars pooled in the cytosol into the lumen of the Golgi and/or the (ER). To analyze whether Slc35f1 plays such a role, we used the glioblastoma cell line U251MG. The cells were transfected with a plasmid expressing tGFP-labeled Slc35f1. Since we expected a localization of slc35f1 in the membrane of ER and or in the membrane of the Golgi apparatus, we searched for a co-labeling of Slc35f1 with markers associated with the ER and Golgi apparatus. However, as shown in Fig. 4, no co-localization of slc35f1 was found with Golgin97, a trans-Golgi network resident protein or with PDIA3 (also known as ERp57), a marker of the ER (Coe and Michalak 2010) was observed. In the central nervous system, Rab proteins, e.g., Rab5, Rab6, and Rab7, play crucial roles in endocytosis and in axonal retrograde transport processes (Ng and Tang 2008). In detail, Rab5 is associated with early endosome fusion, axonal retrograde transport, and endosomal sorting, and Rab7 with processes involving the steps from late endosomes to lysosomes as well as with processes related to axonal retrograde transport (for details, see D'Adamo et al. 2014). Here, we demonstrated that slc35f1 neither co-localizes with Rab5 (Fig. 5a) nor with Rab7 (Fig. 5b), indicating that Slc35f1 is not associated with early or late endosomes. However, we observed that Slc35f1 co-localized with Rab11 (Fig. 5c), a protein that regulates the exocytosis of recycling vesicles (Takahashi et al. 2012). Since Slc35f1 might be involved in Rab11-dependent processes, Slc35f1 might show a dynamic pattern within cells. In Slc35f1-transfected cells, small Slc35f1-positive spots were obvious all over the cell. Time-lapse microscopy of living Slc35f1-transfected cells revealed that these spots are highly dynamic and resemble vesicles as shown in Fig. 6. These dynamic spots move, e.g., in the direction to the cell center (see movie in the supplement). Since the dynamic of the vesicle is dependent on microtubules, we stained with an antibody against α-tubulin to visualize the microtubules system. We found that most of the Slc35f1 spots were associated with the microtubules as shown in Fig. 7.

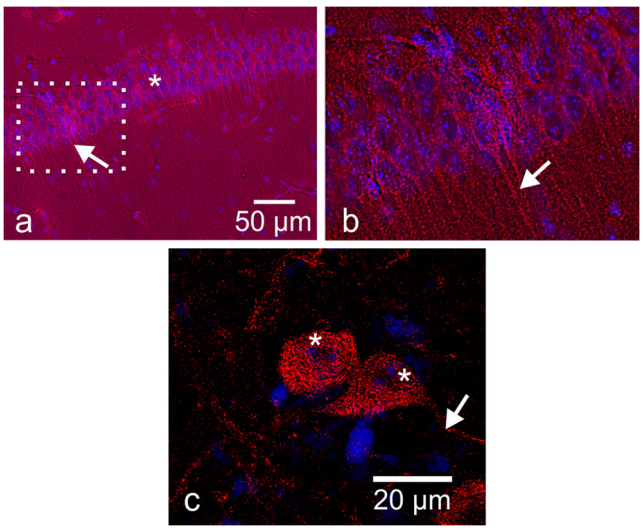

Fig. 3 Slc35f1-positive neurons in the brain. **a** Slc35f1 protein expression (red) is not only seen in the soma (one marked with an asterisk) of CA1 pyramidal neurons but also in the dendrites of neurons (one is marked with an arrow). Rectangle highlights the region of interest shown in (**b**). DAPI (blue) was used to visualize cell nuclei. **b** Magnification of (**a**). The apical dendrites of the CA1 pyramidal neurons display slc35f1 immunoreactivity. **c** By using super-resolution microscopy, the slc35f1 protein expression (red) is now clearly seen in the soma (one marked with an asterisk) as well as in the dendrites of cortical neurons (one is marked with an arrow). DAPI (blue) was used to visualize cell nuclei

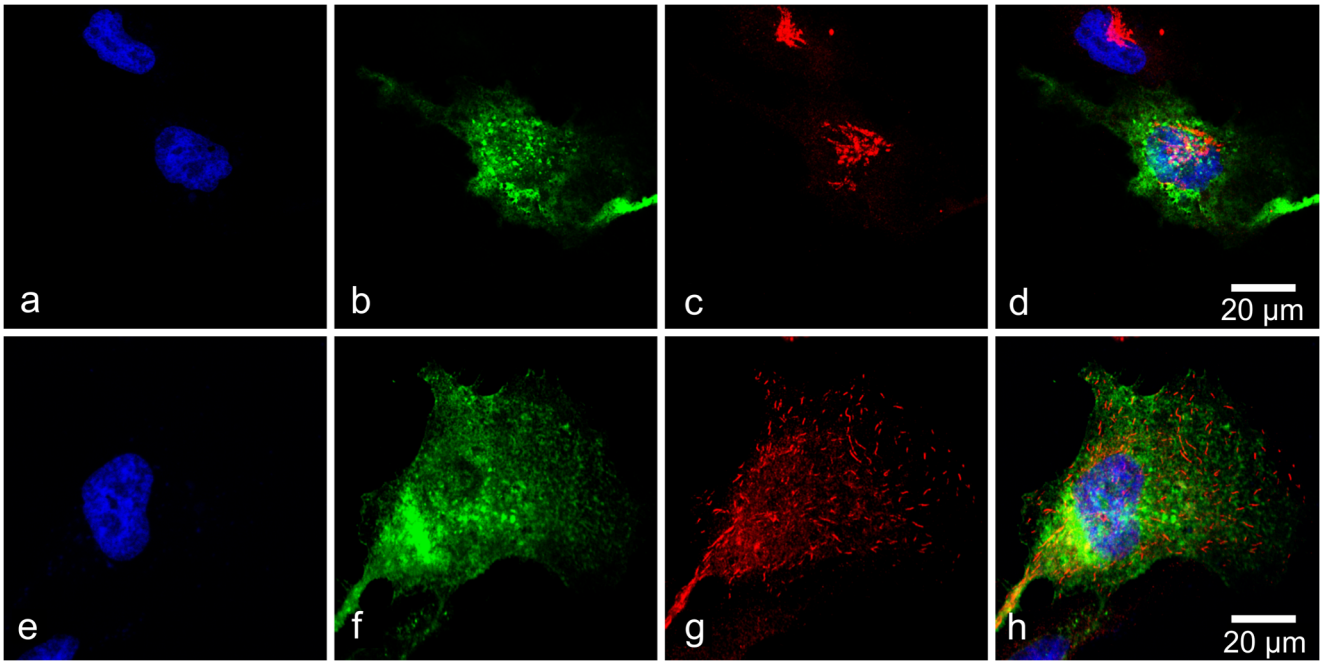

Fig. 4 Slc35f1 does not co-localize with the Golgi apparatus in transfected glioblastoma cells (line U251MG). **a**–**d** tGFP-labeled Slc35f1 and Golgi apparatus co-staining. DAPI staining of cells (**a**) transfected with tGFP-labeled Slc35f1 expression vector (**b**) that were stained with an anti-Golgin97 antibody (red) (**c**), overlay of (**a**), (**b**) and (**c**) (**d**). **e**–**h** tGFP-labeled Slc35f1 and ER co-staining. DAPI staining (**e**) of tGFP-Slc35f1-expressing cells (**f**) that were co-stained with an antibody against PDIA3 (red) (**g**), overlay of (**e**), (**f**) and (**g**) (**h**)

Discussion

In the postnatal murine brain, Slc35f1protein is widely expressed. Slc35f1 protein was mainly seen to be expressed by neurons, but not by astrocytes. Slc35f1 protein expression is not restricted to a specific brain area but can be found in the midbrain, diencephalon, and even in cortical structures, like the basolateral complex of the amygdala, the hippocampal formation, and the cortex. The physiological function of Slc35f1 in the brain, however, is still enigmatic. Based on the localization of Slc35f1 in cortical and hippocampal neurons, it can be speculated that Slc35f1 may be involved in neuronal plasticity or plays a critical role in the maintenance of the neuronal circuitries. Recently, it has been shown that chromosomal 6q22.1 microdeletion is implicated in pediatric epilepsy (Szafranski et al. 2015). The critical region was narrowed to a ~250 kb segment at 6q22.1 that includes, among others, putative regulatory sequences of SLC35F1, indicating that dosage alteration in SLC35F1 may represent important contributors to neurodevelopmental phenotypes associated with 6q22 deletions (Szafranski et al. 2015). As a member of the SLC35 family, SLC35F1 is thought to transport nucleotide sugars pooled in the cytosol into the lumen of the Golgi and/or the ER. In addition, no co-localization of Slc35f1 with markers of the Golgi or ER was seen. Likewise, Slc35f1 was not found to co-localize with the

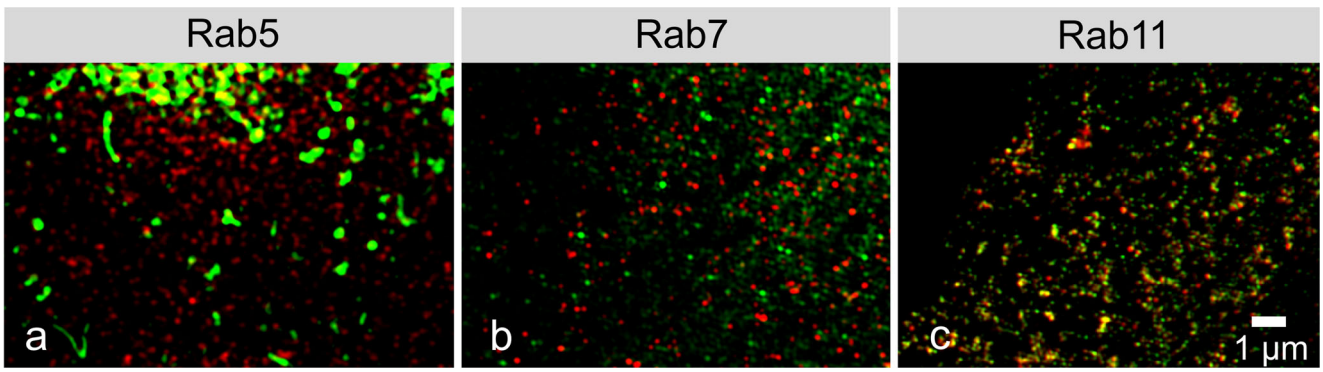

Fig. 5 Slc35f1 and Rab proteins (analysis using transfected glioblastoma cells (line U251MG)). **a** Slc35f1 (labeled in green) and Rab5 (labeled in red) mainly did not co-localize. **b** Slc35f1 (labeled in green) and Rab7 (labeled in red) did not co-localize. **c** Slc35f1 (labeled in green) and Rab11 (labeled in red) were found to co-localize at several positions (seen in yellow)

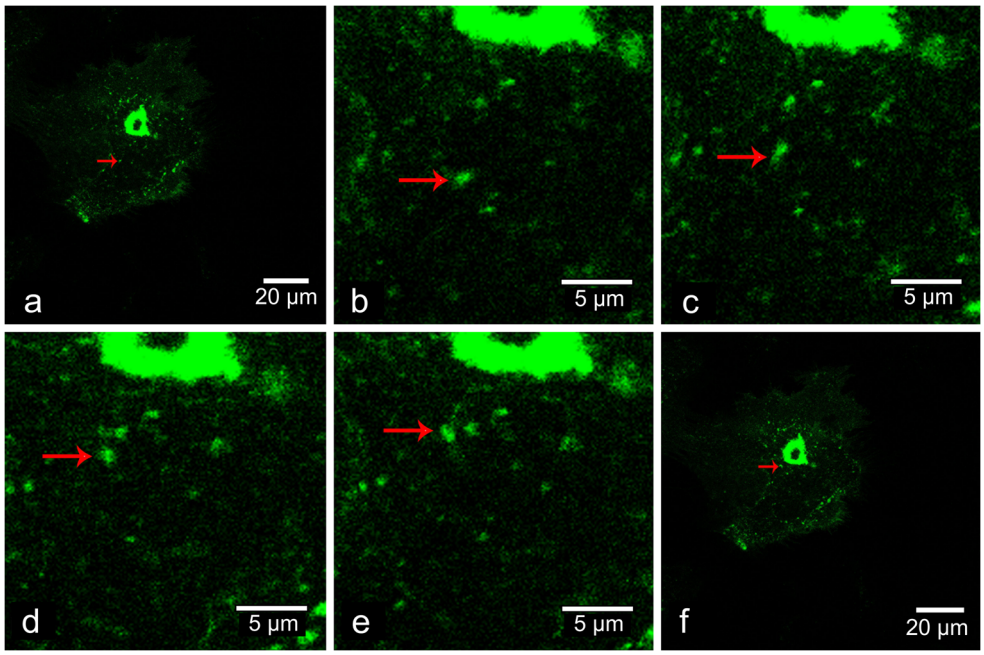

Fig. 6 Dynamics of slc35f1. Glioblastoma cells U251MG transfected with tGFP-SLC35F1 expression vector studied by time-lapse microscopy. **a** Overview and marked starting point. **b**–**e** Magnification of the moving spot that changes the position over the time is marked with a red arrow. **f** Overview and marked end point

endosomal marker Rab5 or Rab7, but, in contrast, Slc35f1 co-localizes with Rab11. Rab11, for example, seems to be required for trans-Golgi network-to-plasma membrane transport (Chen et al. 1998). Rab11-dependent endosomes

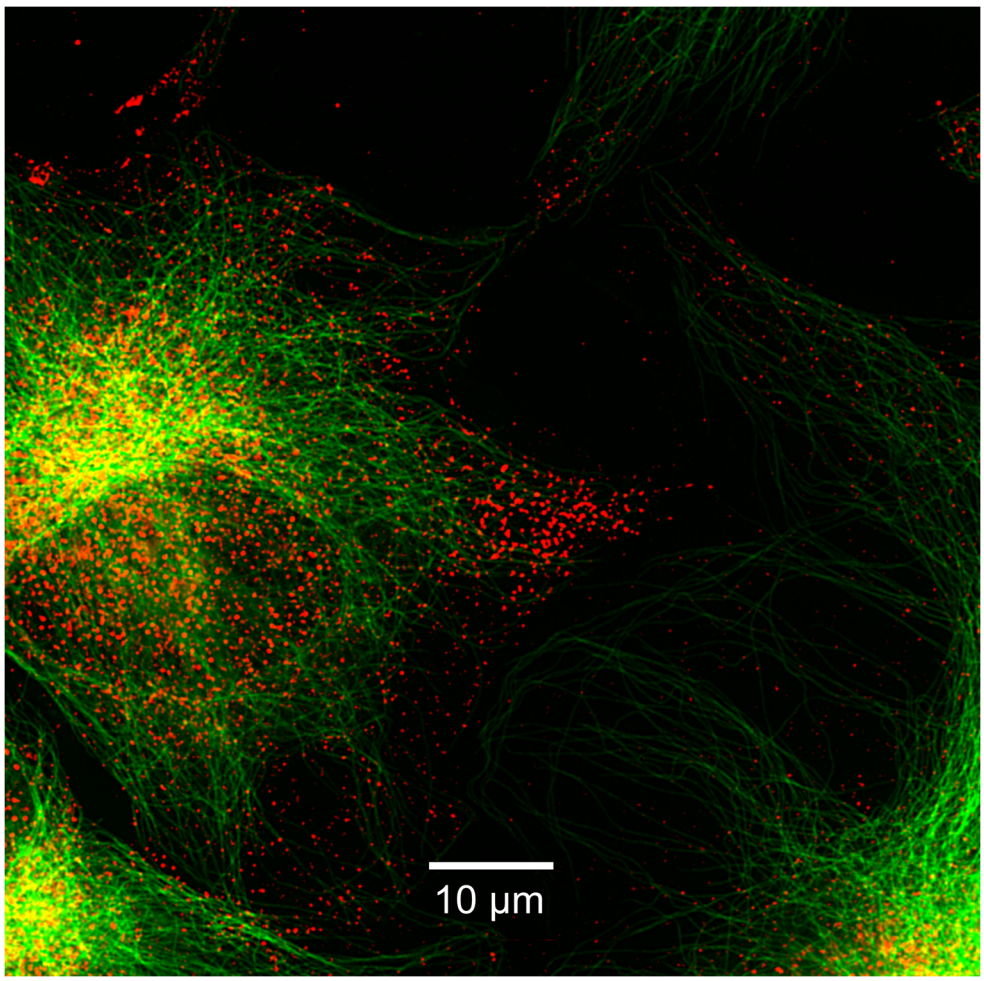

Fig. 7 Slc35f1 spots are associated with microtubules. Overlay of tGFP-labeled slc35f1 spots (red) with α-tubulin staining (green) showed an association with the spots along microtubules in transfected glioblastoma cells

translocate AMPA receptor subunits from the dendritic shaft into spines, e.g., after induction of long-term potentiation (LTP) in the hippocampus (Brown et al. 2007; D'Adamo et al. 2014). Along this line, dominant-negative Rab 11 completely blocks LTP (Brown et al. 2007) and it is known that AMPA receptors play a crucial role in LTP (Payne 2008). Aside from this, altered trafficking and functioning of AMPA receptors are involved in epilepsy (Di Bonaventura et al. 2017). Since Rab11 is involved in the translocation of AMPA receptor subunits from the dendritic shaft into the dendritic spine, Slc35f1, via Rab11, might be involved in dendritic spine formation or in structural changes that depend on synaptic plasticity. Changes in size of dendritic spines are thought to reflect changes in the strength of synaptic transmission under pathophysiological as well as physiological conditions (von Bohlen und Halbach 2009). Thus, it might be possible that Slc35f1 is involved in the highly dynamic processes that may contribute to changes in the size and function of dendritic spines; Slc35f1 should display a dynamic pattern within the cells. Such a dynamic behavior was monitored by time-lapse microscopy of living slc35f1-transfected cells. Slc35f1 seems not to be associated with the ER or the Golgi, but with Rab11-positive endosomes. Importantly, Rab11 is involved in clathrin-mediated endocytosis and has recently been identified as a regulator of presynaptic function especially in activity-dependent bulk endocytosis (ADBE) during high-frequency stimulation (Kokotos et al. 2018). In 2017, a causal link between developmental and epileptic encephalopathy (DEE; a group of conditions characterized by the co-occurrence of epilepsy and intellectual disability), and de-novo missense mutations in several genes, including Rab11 has been discovered (Hamdan et al. 2017). Thus, it can be hypothesized that the possible association of Slc35f1 with epilepsy (Szafranski et al. 2015) may be based on a disturbed Rab11 functioning.

The immunohistochemical analysis of the distribution of Slc35f1 revealed that this protein is expressed by neurons, not only in the soma but also in the dendrites of neurons. Within fiber tracts, e.g., the optical tract, no expression of Slc35f1 was detected. This indicates that Slc35f1 is not expressed in axons as well as it is not expressed by glia cells, e.g., oligodendrocytes. Moreover, we have shown that Slc35f1 does not co-localize with GFAP and, therefore, Slc35f1 is not expressed by astrocytes.

Since the dynamic of the vesicle is dependent on microtubules, we stained with an antibody against α-tubulin to visualize the microtubules system. We found that most of the Slc35f1 spots were associated with the microtubules as shown in Fig. 7. In that context, it should be mentioned that electron microscopic studies have suggested that a highly labile population of microtubules exists within dendritic spines in close proximity to the postsynaptic density (Gu et al. 2008). This presence of microtubules in dendritic spines is correlated with synaptic activity, and brain-derived neurotrophic factor (BDNF) increases the entry of microtubules into dendritic spines (Shirao and Gonzalez-Billault 2013). BDNF also regulates Rab 11-mediated recycling endosome dynamics that leads to structural changes in dendrites (Lazo et al. 2013). It may be possible that Slc35f1 is involved in these processes and it would be interesting to elucidate whether BDNF will have a role in regulating Slc35f1 expression. Moreover, it would be of interest to obtain insight into a possible role of Slc35f1 in synaptic plasticity. The generation of animal models that either over-express or down-regulate Slc35f1 will be very helpful for gaining insight into the roles of Slc35f1 not only in the brain but also in other organs that show high levels of Slc35f1, e.g., the heart or the kidney.

Acknowledgments We thank Sabine Hanisch and Sindy Schröder for excellent technical assistance.

References

Atikuzzaman M, Alvarez-Rodriguez M, Vicente-Carrillo A, Johnsson M, Wright D, Rodriguez-Martinez H (2017) Conserved gene expression in sperm reservoirs between birds and mammals in response to mating. BMC Genomics 18:98

Avery CL, Wassel CL, Richard MA, Highland HM, Bien S, Zubair N, Soliman EZ, Fornage M, Bielinski SJ, Tao R, Seyerle AA, Shah SJ, Lloyd-Jones DM, Buyske S, Rotter JI, Post WS, Rich SS, Hindorff LA, Jeff JM, Shohet RV, Sotoodehnia N, Lin DY, Whitsel EA, Peters U, Haiman CA, Crawford DC, Kooperberg C, North KE (2017) Fine mapping of QT interval regions in global populations refines previously identified QT interval loci and identifies signals unique to African and Hispanic descent populations. Heart Rhythm 14:572–580

Blumenthal A, Giebel J, Warsow G, Li L, Ummanni R, Schordan S, Schordan E, Klemm P, Gretz N, Endlich K, Endlich N (2015) Mechanical stress enhances CD9 expression in cultured podocytes. Am J Physiol Ren Physiol 308:F602–F613

Brown TC, Correia SS, Petrok CN, Esteban JA (2007) Functional compartmentalization of endosomal trafficking for the synaptic delivery of AMPA receptors during long-term potentiation. J Neurosci 27: 13311–13315

Busch R, Baldus M, Vogt M, Berger S, Bartsch D, Gass P, von Bohlen und Halbach O (2017) Effects of p75NTR-deficiency on cholinergic innervation of the amygdala and anxiety-like behavior. J Neurochem 141:461–471

Chen W, Feng Y, Chen D, Wandinger-Ness A (1998) Rab11 is required for trans-golgi network-to-plasma membrane transport and a preferential target for GDP dissociation inhibitor. Mol Biol Cell 9:3241–3257

Coe H, Michalak M (2010) ERp57, a multifunctional endoplasmic reticulum resident oxidoreductase. Int J Biochem Cell Biol 42:796–799

Creeley CE, Olney JW (2010) The young: neuroapoptosis induced by anesthetics and what to do about it. Anesth Analg 110:442–448

D'Adamo P, Masetti M, Bianchi V, More L, Mignogna ML, Giannandrea M, Gatti S (2014) RAB GTPases and RAB-interacting proteins and their role in the control of cognitive functions. Neurosci Biobehav Rev 46(Pt 2):302–314

Di Bonaventura C, Labate A, Maschio M, Meletti S, Russo E (2017) AMPA receptors and perampanel behind selected epilepsies: current evidence and future perspectives. Expert Opin Pharmacother 18: 1751–1764

Dokter M, Busch R, Poser R, Vogt MA, von Bohlen und Halbach V, Gass P, Unsicker K, von Bohlen und Halbach O (2015) Implications of p75NTR for dentate gyrus morphology and hippocampus-related behavior revisited. Brain Struct Funct 220:1449–1462

Eijgelsheim M, Newton-Cheh C, Sotoodehnia N, de Bakker PI, Muller M, Morrison AC, Smith AV, Isaacs A, Sanna S, Dorr M, Navarro P, Fuchsberger C, Nolte IM, de Geus EJ, Estrada K, Hwang SJ, Bis JC, Ruckert IM, Alonso A, Launer LJ, Hottenga JJ, Rivadeneira F, Noseworthy PA, Rice KM, Perz S, Arking DE, Spector TD, Kors JA, Aulchenko YS, Tarasov KV, Homuth G, Wild SH, Marroni F, Gieger C, Licht CM, Prineas RJ, Hofman A, Rotter JI, Hicks AA, Ernst F, Najjar SS, Wright AF, Peters A, Fox ER, Oostra BA, Kroemer HK, Couper D, Volzke H, Campbell H, Meitinger T, Uda M, Witteman JC, Psaty BM, Wichmann HE, Harris TB, Kaab S, Siscovick DS, Jamshidi Y, Uitterlinden AG, Folsom AR, Larson MG, Wilson JF, Penninx BW, Snieder H, Pramstaller PP, van Duijn CM, Lakatta EG, Felix SB, Gudnason V, Pfeufer A, Heckbert SR, Stricker BH, Boerwinkle E, O'Donnell CJ (2010) Genome-wide association analysis identifies multiple loci related to resting heart rate. Hum Mol Genet 19:3885–3894

Franklin K, Paxinos G (2008) The mouse brain in stereotaxic coordinates, 3rd edn. Academic Press, Cambridge

Freund M, Walther T, von Bohlen und Halbach O (2012) Immunohistochemical localization of the angiotensin-(1-7) receptor Mas in the murine forebrain. Cell Tissue Res 348:29–35

Gebhardt C, von Bohlen und Halbach O, Hadler MD, Harteneck C, Albrecht D (2016) A novel form of capsaicin-modified amygdala LTD mediated by TRPM1. Neurobiol Learn Mem 136:1–12

Gu J, Firestein BL, Zheng JQ (2008) Microtubules in dendritic spine development. J Neurosci 28:12120–12124

Hamdan FF, Myers CT, Cossette P, Lemay P, Spiegelman D, Laporte AD, Nassif C, Diallo O, Monlong J, Cadieux-Dion M, Dobrzeniecka S, Meloche C, Retterer K, Cho MT, Rosenfeld JA, Bi W, Massicotte C, Miguet M, Brunga L, Regan BM, Mo K, Tam C, Schneider A, Hollingsworth G, Deciphering Developmental Disorders S, FitzPatrick DR, Donaldson A, Canham N, Blair E, Kerr B, Fry AE, Thomas RH, Shelagh J, Hurst JA, Brittain H, Blyth M, Lebel RR, Gerkes EH, Davis-Keppen L, Stein Q, Chung WK, Dorison SJ, Benke PJ, Fassi E, Corsten-Janssen N, Kamsteeg EJ, Mau-Them FT, Bruel AL, Verloes A, Ounap K, Wojcik MH, Albert DVF, Venkateswaran S, Ware T, Jones D, Liu YC, Mohammad SS, Bizargity P, Bacino CA, Leuzzi V, Martinelli S, Dallapiccola B, Tartaglia M, Blumkin L, Wierenga KJ, Purcarin G, O'Byrne JJ, Stockler S, Lehman A, Keren B, Nougues MC, Mignot C, Auvin S, Nava C, Hiatt SM, Bebin M, Shao Y, Scaglia F, Lalani SR, Frye RE, Jarjour IT, Jacques S, Boucher RM, Riou E, Srour M, Carmant L, Lortie A, Major P, Diadori P, Dubeau F, D'Anjou G, Bourque G, Berkovic SF, Sadleir LG, Campeau PM, Kibar Z, Lafreniere RG, Girard SL, Mercimek-Mahmutoglu S, Boelman C, Rouleau GA, Scheffer IE, Mefford HC, Andrade DM, Rossignol E, Minassian BA, Michaud JL (2017) High rate of recurrent de novo mutations in developmental and epileptic encephalopathies. Am J Hum Genet 101:664–685

Hediger MA, Clemencon B, Burrier RE, Bruford EA (2013) The ABCs of membrane transporters in health and disease (SLC series): introduction. Mol Asp Med 34:95–107

Ishida N, Kawakita M (2004) Molecular physiology and pathology of the nucleotide sugar transporter family (SLC35). Pflugers Arch 447: 768–775

Kasukurthi R, Brenner MJ, Moore AM, Moradzadeh A, Ray WZ, Santosa KB, Mackinnon SE, Hunter DA (2009) Transcardial perfusion versus immersion fixation for assessment of peripheral nerve regeneration. J Neurosci Methods 184:303–309

Kokotos AC, Peltier J, Davenport EC, Trost M, Cousin MA (2018) Activity-dependent bulk endocytosis proteome reveals a key presynaptic role for the monomeric GTPase Rab11. Proc Natl Acad Sci U S A 115:E10177–E10186

Koschützke L, Bertram J, Hartmann B, Bartsch D, Lotze M, von Bohlen und Halbach O (2015) SrGAP3 knockout mice display enlarged lateral ventricles and specific cilia disturbances of ependymal cells in the third ventricle. Cell Tissue Res 361:645–650

Lazo OM, Gonzalez A, Ascano M, Kuruvilla R, Couve A, Bronfman FC (2013) BDNF regulates Rab11-mediated recycling endosome dynamics to induce dendritic branching. J Neurosci 33:6112–6122

Ng EL, Tang BL (2008) Rab GTPases and their roles in brain neurons and glia. Brain Res Rev 58:236–246

Nishimura M, Suzuki S, Satoh T, Naito S (2009) Tissue-specific mRNA expression profiles of human solute carrier 35 transporters. Drug Metab Pharmacokinet 24:91–99

Payne HL (2008) The role of transmembrane AMPA receptor regulatory proteins (TARPs) in neurotransmission and receptor trafficking (review). Mol Membr Biol 25:353–362

Sall JW, Stratmann G, Leong J, McKleroy W, Mason D, Shenoy S, Pleasure SJ, Bickler PE (2009) Isoflurane inhibits growth but does not cause cell death in hippocampal neural precursor cells grown in culture. Anesthesiology 110:826–833

Shirao T, Gonzalez-Billault C (2013) Actin filaments and microtubules in dendritic spines. J Neurochem 126:155–164

Siegerist F, Ribback S, Dombrowski F, Amann K, Zimmermann U, Endlich K, Endlich N (2017) Structured illumination microscopy and automatized image processing as a rapid diagnostic tool for podocyte effacement. Sci Rep 7:11473

Song Z (2013) Roles of the nucleotide sugar transporters (SLC35 family) in health and disease. Mol Asp Med 34:590–600

Stratmann G, Sall JW, May LD, Bell JS, Magnusson KR, Rau V, Visrodia KH, Alvi RS, Ku B, Lee MT, Dai R (2009) Isoflurane differentially affects neurogenesis and long-term neurocognitive function in 60-day-old and 7-day-old rats. Anesthesiology 110:834–848

Szafranski P, Von Allmen GK, Graham BH, Wilfong AA, Kang SH, Ferreira JA, Upton SJ, Moeschler JB, Bi W, Rosenfeld JA, Shaffer LG, Wai Cheung S, Stankiewicz P, Lalani SR (2015) 6q22.1 microdeletion and susceptibility to pediatric epilepsy. Eur J Hum Genet 23:173–179

Takahashi S, Kubo K, Waguri S, Yabashi A, Shin HW, Katoh Y, Nakayama K (2012) Rab11 regulates exocytosis of recycling vesicles at the plasma membrane. J Cell Sci 125:4049–4057

Vasan RS, Glazer NL, Felix JF, Lieb W, Wild PS, Felix SB, Watzinger N, Larson MG, Smith NL, Dehghan A, Grosshennig A, Schillert A, Teumer A, Schmidt R, Kathiresan S, Lumley T, Aulchenko YS, Konig IR, Zeller T, Homuth G, Struchalin M, Aragam J, Bis JC, Rivadeneira F, Erdmann J, Schnabel RB, Dorr M, Zweiker R, Lind L, Rodeheffer RJ, Greiser KH, Levy D, Haritunians T, Deckers JW, Stritzke J, Lackner KJ, Volker U, Ingelsson E, Kullo I, Haerting J, O'Donnell CJ, Heckbert SR, Stricker BH, Ziegler A, Reffelmann T, Redfield MM, Werdan K, Mitchell GF, Rice K, Arnett DK, Hofman A, Gottdiener JS, Uitterlinden AG, Meitinger T, Blettner M, Friedrich N, Wang TJ, Psaty BM, van Duijn CM, Wichmann HE, Munzel TF, Kroemer HK, Benjamin EJ, Rotter JI, Witteman JC, Schunkert H, Schmidt H, Volzke H, Blankenberg S (2009) Genetic variants associated with cardiac structure and function: a meta-analysis and replication of genome-wide association data. JAMA 302:168–178

von Bohlen und Halbach O (2009) Structure and function of dendritic spines within the hippocampus. Ann Anat 191:518–531

Zschenderlein C, Gebhardt C, von Bohlen und Halbach O, Kulisch C, Albrecht D (2011) Capsaicin-induced changes in LTP in the lateral amygdala are mediated by TRPV1. PLoS One 6:e16116